

## Scattering of light by a parity-time-symmetric dipole beyond the first Born approximation

J. A. Rebouças <sup>\*</sup>

*Instituto Federal de Educação, Ciência e Tecnologia do Ceará, Iguatu, Ceará 63500-000, Brazil  
and Universidade Federal de Alagoas, Maceió, Alagoas 57072-900, Brazil*

P. A. Brandão 

*Universidade Federal de Alagoas, Maceió, Alagoas 57072-900, Brazil*



(Received 6 October 2021; revised 26 November 2021; accepted 2 December 2021; published 17 December 2021)

The scattering of light by localized three-dimensional dielectrics having gain and loss defies the usual Born approximation, since the material can increase the amplitude of the incident field within the scatterer, making the weak-scattering assumption invalid. The convergence of the Born series is rarely discussed in analytical treatments, as the state of exhaustion is reached after calculating the very first few terms of the series. Even if all the terms are obtained, the series will certainly be of a divergent type in general, thus invalidating the equality of the scattered field to its Taylor-series representation. We present here a simple localized material model of a dielectric having parity-time ( $\mathcal{PT}$ ) symmetry, consisting of a  $\mathcal{PT}$ -symmetric dipole, such that all the terms in the Born series are analytically evaluated and a closed-form expression is obtained in the far-zone approximation. The scattered field is then analyzed by using Padé approximants in order to obtain convergent representations of the scattered radiation and to compare with the exact solution. This allows us to study the role of the gain and loss parameter in strong-scattering regimes and to demonstrate the remarkable properties of Padé approximants when applied to scattering.

DOI: [10.1103/PhysRevA.104.063514](https://doi.org/10.1103/PhysRevA.104.063514)

### I. INTRODUCTION

The scattering of radiation by dielectrics is one of the most important techniques available to obtain information about the inner structure of unknown objects and also to control the scattered wave field emanating from known dielectric material distributions. The mathematical theory behind it is very rich and has many levels of sophistication that permeates almost every field of physics [1]. In one of these ramifications, approximate solutions can be found by using perturbation theory. The idea is to represent the total field as a power-series expansion (Taylor series) in terms of some parameter such that if this parameter is set to zero, one obtains the solution to the unperturbed problem, representing the system without a scatterer. The advantage of this representation is that the coefficients of the Taylor series are usually easy to obtain, at least for the first few terms, and one hopes that they represent a good approximation to the exact answer as long as the expansion parameter is small in some sense (weak scattering) [2–10].

The disadvantage is that in some cases one is willing to obtain information in strong-scattering regimes, where the material strongly interacts with the incident radiation. If the Taylor representation is the only tool available, a large number of terms must be computed to obtain accurate results. This procedure is certainly to be done using computers and numerical approximations. Furthermore, the radius of convergence

in the power-series representation may not be easy to obtain since the analytical formula for all coefficients in the expansion is generally unknown. Even if the convergence radius is known, the physically reasonable numerical parameters can be such that the series diverges. Another representation which has been proven to be very useful arises if we replace the partial sums of the Taylor terms by Padé approximants. In this case, the function being sought is represented by a fraction of two polynomials [11–13]. There has been some work involving Padé approximants in quantum scattering theory [14–18] and in classical electromagnetic scattering [19,20]. Our approach closely follows a recent treatment involving one- and two-dimensional scattering with lossy materials [21].

Since the initial exposition of the remarkable effects of parity-time ( $\mathcal{PT}$ ) symmetry [22,23] in optics [24–31], the scattering of light by non-Hermitian materials with gain and loss has developed a new twist. In one-dimensional systems, effects such as unidirectional reflectionless materials [32] and the  $\mathcal{PT}$ -symmetric laser absorber [33] are among the most drastic ones highlighting the non-Hermitian aspect of photonics. In these one-dimensional systems possessing homogeneous material layers, the transfer and scattering matrix formalism are the most suited to obtain exact results for the transmittance and reflectance amplitudes [34]. However, in three-dimensional settings the lack of a general formalism forces us to deal with the Born series and the problem of its convergence. This is especially important if the material has gain because it could invalidate the weak-scattering assumption (first Born approximation).

\*jalvesreboucas@gmail.com

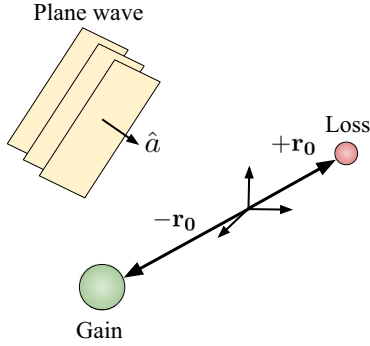


FIG. 1. Scattering system. A monochromatic plane wave of frequency  $\omega$  traveling in the direction specified by the unit vector  $\hat{a}$  interacts with the scatterer composed of two point particles with gain and loss ( $\mathcal{PT}$ -symmetric dipole). The position of the particle with loss (gain) is  $+\mathbf{r}_0$  ( $-\mathbf{r}_0$ ). All quantities plotted have arbitrary units.

Our aim here is to demonstrate how the Born series can be directly summed to obtain the exact closed-form solution to a three-dimensional scattering problem with a scatterer described by a  $\mathcal{PT}$ -symmetric physical dipole (see Fig. 1). This exact solution allows us to study the behavior of the scattered radiation in strong-scattering regimes. With the analytical solution at our disposal, the Padé representation of the scattered field is analyzed in order to highlight its remarkable properties over the Taylor-series representation. In Sec. II we present the general scattering formalism for a scalar field, the Born series, and the exact closed-form solution to the scattering of light by a  $\mathcal{PT}$ -symmetric dipole. Section III is devoted to a detailed discussion of Taylor and Padé approximants to the scattered field amplitude and its relation to the gain and loss parameter present in the scatterer. In Sec. IV we present a summary and our conclusions.

## II. SCATTERING THEORY AND BORN SERIES

Consider the scalar representation of a complex optical wave field  $u(\mathbf{r}, \omega)$  of monochromatic angular frequency  $\omega$  satisfying the differential equation

$$\nabla^2 u(\mathbf{r}, \omega) + k^2 \varepsilon(\mathbf{r}, \omega) u(\mathbf{r}, \omega) = 0, \quad (1)$$

where  $k = \omega/c$  is the wave number, with  $c$  the speed of light in vacuum, and  $\varepsilon(\mathbf{r}, \omega)$  represents the complex-valued relative permittivity of a localized scatterer. By writing the relative permittivity as  $\varepsilon(\mathbf{r}, \omega) = 1 + \alpha \chi(\mathbf{r}, \omega)$ , with  $\chi(\mathbf{r}, \omega)$  the linear electric susceptibility and  $\alpha$  the perturbation parameter, the differential equation satisfied by the wave field  $u(\mathbf{r}, \omega)$  is given by

$$\nabla^2 u(\mathbf{r}, \omega) + k^2 u(\mathbf{r}, \omega) = -\alpha k^2 \chi(\mathbf{r}, \omega) u(\mathbf{r}, \omega). \quad (2)$$

The original problem we want to solve is recovered by setting  $\alpha = 1$ . To obtain the integral form of Eq. (2), we view the right-hand side as an inhomogeneous term and define the Green's function  $G(\mathbf{r}, \mathbf{r}') = G(\mathbf{r} - \mathbf{r}')$  as a solution of

$$\nabla^2 G(\mathbf{r} - \mathbf{r}') + k^2 G(\mathbf{r} - \mathbf{r}') = -\delta(\mathbf{r} - \mathbf{r}') \quad (3)$$

such that it is possible to write

$$u(\mathbf{r}) = u_0(\mathbf{r}) + \alpha k^2 \int_{r'} \chi(\mathbf{r}') u(\mathbf{r}') G(\mathbf{r} - \mathbf{r}') d^3 r', \quad (4)$$

where  $u_0(\mathbf{r})$  is the solution to the homogeneous equation, which is obtained from (2) with  $\alpha = 0$  (unperturbed problem). The explicit form of the Green's function  $G(\mathbf{r} - \mathbf{r}')$  that is physically acceptable is given by

$$G(\mathbf{r} - \mathbf{r}') = \frac{e^{ik|\mathbf{r}-\mathbf{r}'|}}{4\pi|\mathbf{r} - \mathbf{r}'|}. \quad (5)$$

To apply perturbation methods, we assume that the field can be expressed as a power series in  $\alpha$ ,

$$u(\mathbf{r}) = \sum_{n=0}^{\infty} u_n(\mathbf{r}) \alpha^n, \quad (6)$$

where  $u_0(\mathbf{r})$  is the solution to the unperturbed problem with  $\alpha = 0$ . Equation (6) is known as the Born series. The unperturbed wave field  $u_0(\mathbf{r})$  satisfies the homogeneous Helmholtz equation  $\nabla^2 u_0(\mathbf{r}) + k^2 u_0(\mathbf{r}) = 0$  and represents the total field in the absence of the scatterer. We assume that the unperturbed wave field is given by the plane wave

$$u_0(\mathbf{r}) = e^{ik\hat{a}\cdot\mathbf{r}}, \quad (7)$$

where  $\hat{a}$  is a unit vector indicating the incident direction.

After substituting Eq. (6) into (4), we obtain the recursion relation between the expansion coefficients  $u_n(\mathbf{r})$ :

$$u_n(\mathbf{r}) = k^2 \int_{r'} \chi(\mathbf{r}') G(|\mathbf{r} - \mathbf{r}'|) u_{n-1}(\mathbf{r}') d^3 r' \quad (n \geq 1). \quad (8)$$

The first correction  $u_1(\mathbf{r})$  to the total field  $u(\mathbf{r})$  is known as the Born approximation. In what follows, we will be interested in the scattered field far beyond the region where the scatterer is located (far-zone approximation). Therefore, the Green's function represented by Eq. (5) can be approximated by

$$\frac{e^{ik|\mathbf{r}-\mathbf{r}'|}}{4\pi|\mathbf{r} - \mathbf{r}'|} \sim \frac{e^{ikr}}{4\pi r} e^{-ik\hat{s}\cdot\mathbf{r}'} \quad (r \gg r'), \quad (9)$$

where  $\hat{s} = \mathbf{r}/r$  and  $r = |\mathbf{r}|$ .

The localized material is represented by a  $\mathcal{PT}$ -symmetric dipole, given by the dielectric constant  $\varepsilon(\mathbf{r}, \omega) = 1 + \alpha \chi(\mathbf{r}, \omega)$ , with the linear electric susceptibility  $\chi(\mathbf{r}, \omega)$  written as

$$\chi(\mathbf{r}, \omega) = (\sigma + i\gamma)\delta(\mathbf{r} - \mathbf{r}_0) + (\sigma - i\gamma)\delta(\mathbf{r} + \mathbf{r}_0), \quad (10)$$

where  $\sigma$  and  $\gamma$  are positive parameters and  $+\mathbf{r}_0$  ( $-\mathbf{r}_0$ ) is the position of the scatterer which has loss (gain) [35,36]. After substituting Eqs. (9) and (10) into (8) we obtain

$$u_n(\mathbf{r}) = \frac{k^2}{4\pi} \frac{e^{ikr}}{r} \left[ (\sigma + i\gamma) u_{n-1}(\mathbf{r}_0) e^{-ik\hat{s}\cdot\mathbf{r}_0} + (\sigma - i\gamma) u_{n-1}(-\mathbf{r}_0) e^{ik\hat{s}\cdot\mathbf{r}_0} \right] \quad (n = 1, 2, 3, \dots). \quad (11)$$

Since we are interested in the scattered field amplitude, it is more convenient to write the total field

as

$$\begin{aligned}
 u(\mathbf{r}) &= u_0(\mathbf{r}) + u_1(\mathbf{r})\alpha + u_2(\mathbf{r})\alpha^2 + \dots \\
 &= u_0(\mathbf{r}) + \frac{e^{ikr}}{r} [\tilde{u}_1(\mathbf{r})\alpha + \tilde{u}_2(\mathbf{r})\alpha^2 + \dots] \\
 &= u_0(\mathbf{r}) + \frac{e^{ikr}}{r} \tilde{u}_s(\mathbf{r}), \tag{12}
 \end{aligned}$$

where  $\tilde{u}_s(\mathbf{r})$  is the scattering amplitude, and deal directly with  $\tilde{u}_i(\mathbf{r})$ , which is independent of  $r$ . In the Appendix we demonstrate the induction process employed to obtain a closed-form expression for  $\tilde{u}_n(\mathbf{r})$  and  $\tilde{u}_s(\mathbf{r})$ . Although the expressions are a bit involved, this is a rare example where the  $n$ th term of the expansion can be written analytically for a scattering three-dimensional problem. The closed-form expression for  $\tilde{u}_s$  is given by

$$\begin{aligned}
 \tilde{u}_s(\mathbf{r}) &= e^{-ik\hat{s}\cdot\mathbf{r}_0} \\
 &\times \frac{-D_2k^4Q_0 + D_4k^4P_0 - 4\pi k^2P_0}{D_2D_3k^4 - (D_1k^2 - 4\pi)(D_4k^2 - 4\pi)} \\
 &+ e^{ik\hat{s}\cdot\mathbf{r}_0} \frac{D_1k^4Q_0 - D_3k^4P_0 - 4\pi k^2Q_0}{D_2D_3k^4 - (D_1k^2 - 4\pi)(D_4k^2 - 4\pi)}, \tag{13}
 \end{aligned}$$

where  $P_0 = (\sigma + i\gamma)e^{ik\hat{a}\cdot\mathbf{r}_0}$ ,  $Q_0 = (\sigma - i\gamma)e^{-ik\hat{a}\cdot\mathbf{r}_0}$ ,  $D_1 = (\sigma + i\gamma)/r_0$ ,  $D_2 = (\sigma + i\gamma)e^{2ki r_0}/r_0$ ,  $D_3 = (\sigma - i\gamma)e^{2ki r_0}/r_0$ , and  $D_4 = (\sigma - i\gamma)/r_0$ . One final quantity that will be of interest is the partial sum  $S_N$  of the first  $N$  terms in the Taylor-series representation,  $S_N(\mathbf{r}) = \sum_{n=1}^N \tilde{u}_n(\mathbf{r})$ , with  $S_1(\mathbf{r})$  the scattering amplitude in the usual Born approximation. In the next section we discuss the relationship between the closed-form expression for  $\tilde{u}_s(\mathbf{r})$  and the correction terms  $\tilde{u}_n$  along with its Padé approximants for the scattered radiation.

### III. TAYLOR AND PADÉ REPRESENTATIONS FOR THE SCATTERED FIELD

This section is devoted to a more detailed discussion involving the exact solution obtained in the preceding section and its connection to Taylor and Padé representations. The following discussion is divided between passive scatterers with  $\gamma = 0$  (Hermitian scattering) and active scatterers with  $\gamma \neq 0$  (non-Hermitian scattering).

#### A. Hermitian scattering

Consider the situation without the presence of gain and/or loss in the scatterers, i.e.,  $\gamma = 0$ . An important issue to be addressed is how the scattering amplitude, in a fixed direction  $(\theta, \phi)$ , behaves as we increase  $\sigma$ , thus making the transition between weak- and strong-scattering regimes. The exact answer to this question cannot be obtained if one is working with the first Born approximation since, in this case, the scattering amplitude is a linear function of  $\sigma$  and so it predicts an infinite amplitude in the limit  $\sigma \rightarrow \infty$ :

$$S_1(\mathbf{r}) = \tilde{u}_1(\mathbf{r}) = \sigma \frac{k^2}{2\pi} \cos[k\mathbf{r}_0 \cdot (\hat{a} - \hat{s})]. \tag{14}$$

Figure 2 shows the plot of  $|S_1(\mathbf{r})|$  (first Born approximation) as a function of  $\sigma$  for a fixed scattering direction (dashed

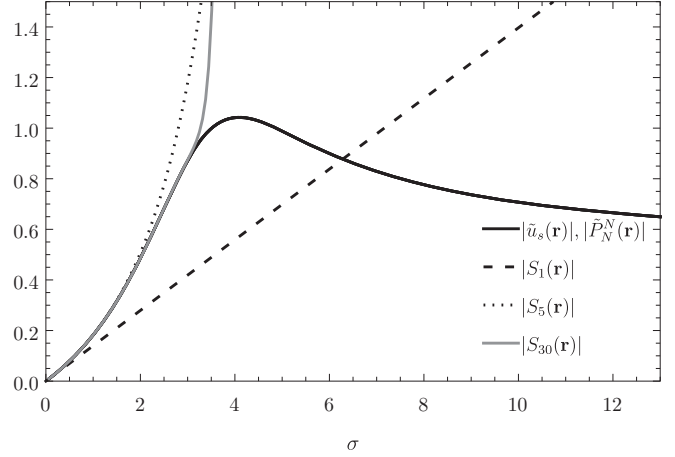


FIG. 2. Scattered field amplitude as a function of  $\sigma$ . The dashed line shows the first Born approximation  $|S_1(\mathbf{r})|$ , the dotted line  $|S_5(\mathbf{r})|$ , the gray solid line  $|S_{30}(\mathbf{r})|$ , and the black solid line  $|\tilde{u}_s(\mathbf{r})|$  ( $N = 1, 2, 3$ ) and the exact solution  $|\tilde{u}_s(\mathbf{r})|$ . For more information see Table II. The parameters are  $\theta = \frac{\pi}{2}$ ,  $\phi = 0$ ,  $k = 1$ ,  $x_0 = \frac{1}{2}$ , and  $\gamma = 0$ . All quantities plotted have arbitrary units.

curve). The picture also shows the plots of the sum of the first 5 and 30 terms in the Taylor series,  $|S_5(\mathbf{r})|$  (dotted curve) and  $|S_{30}(\mathbf{r})|$  (gray solid line) along with the exact solution for  $|\tilde{u}_s(\mathbf{r})|$  (black curve). Curiously, as we increase  $\sigma$ , the field amplitude increases and it reaches a maximum value around  $\sigma \approx 4$  before it saturates to a constant amplitude. As expected, we obtain better accuracy as we add more terms into the Taylor partial sum. Notice, however, that the discrepancy between the first Born approximation and the exact solution is very pronounced even for small values of  $\sigma$ . To explain the behavior of the partial sums displayed in Fig. 2, we calculate the radius of convergence of the Born series in the complex  $\alpha$  plane. The first column of Table I shows several values of  $\sigma$  and  $R_\alpha$  is the convergence radius for the respective values of  $\sigma$ . Since the original problem is restored by choosing  $\alpha = 1$ , Table I indicates that the Taylor series diverges for  $\sigma > 3.57983$ , approximately. Since the Taylor representation is not suitable to obtain information in strong-scattering regimes, we turn our discussion to another representation. A

TABLE I. Radius of convergence  $R_\alpha$  in the complex  $\alpha$  plane for the Taylor series  $\sum_n u_n \alpha^n$  for several values of  $\sigma$ . The parameters are  $\phi = 0$ ,  $\theta = \frac{\pi}{2}$ ,  $k = 1$ ,  $x_0 = \frac{1}{2}$ , and  $\gamma = 0$ .

$\sigma$	$R_\alpha$
1	3.57983
2	1.78991
3	1.19328
4	0.894956
5	0.715965
6	0.596638
7	0.511404
8	0.447478
9	0.397758
10	0.357983

TABLE II. Comparison between the exact solution  $\tilde{u}_s$  for the scattered field amplitude and its Taylor  $S_N$  and Padé  $\tilde{P}_N^N$  representations (with  $\sigma = 1$ ). The parameters are  $\gamma = 0$ ,  $k = 1$ ,  $x_0 = \frac{1}{2}$ ,  $\phi = 0$ , and  $\theta = \frac{\pi}{2}$ . All values of  $\alpha$  are inside the radius of convergence.

$\alpha$	Exact solution	$ S_N  (N)$	$ \tilde{P}_1^1 $	$ \tilde{P}_2^2 $
3.57	1.0090898257861656	1.0090877280387027(4000)	1.0090898257861698	1.009089825786168
1.79	0.40969141139798726	0.40969141139798715(100)	0.4096914113979872	0.40969141139798704
0.895	0.15828711442382187	0.15828711442382182(30)	0.15828711442382185	0.1582871144238218
0.447	0.06995869702491307	0.06995869702491307(20)	0.06995869702491307	0.0699586970249131
0.0357	0.0050302415730227356	0.005030241573022735(10)	0.0050302415730227356	0.005030241573022735

Padé approximant  $P_M^N$  of order  $(M, N)$  is defined as the ratio between two polynomials with degrees  $M$  and  $N$ ,

$$P_M^N(\mathbf{r}) = \frac{\sum_{n=0}^N A_n(\mathbf{r})\alpha^n}{\sum_{m=0}^M B_m(\mathbf{r})\alpha^m}, \quad (15)$$

where we define  $B_0 = 1$  without loss of generality. The remaining  $M + N + 1$  coefficients  $A_n$  and  $B_n$  are related to  $u_n$  of Eq. (6) after the first  $M + N + 1$  terms in the Taylor-series expansion of  $P_M^N$  match the first  $M + N + 1$  terms of the power series (6). There are well-known algorithms to efficiently perform such operations [11,13]. In what follows, we only consider the diagonal approximants with  $M = N$ . We have performed numerical simulations (not shown) and verified that the off-diagonal approximants  $P_M^{M+1}$  and  $P_{M+1}^M$  indeed converge to the exact answer in the appropriate limit.

As an elementary example, the approximant  $P_1^1(\mathbf{r})$  is given explicitly by

$$\begin{aligned} P_1^1(\mathbf{r}) &= \frac{A_0(\mathbf{r}) + A_1(\mathbf{r})\alpha}{1 + B_1(\mathbf{r})\alpha} \\ &= u_0(\mathbf{r}) + \frac{u_1^2(\mathbf{r})\alpha}{u_1(\mathbf{r}) - u_2(\mathbf{r})\alpha}. \end{aligned} \quad (16)$$

Thus, to obtain  $P_N^N(\mathbf{r})$  we need the first  $2N + 1$  coefficients in the Taylor representation. Our claim is that the approximants approach the correct answer as  $N$  increases. We discuss this point later.

All diagonal approximants are of the form  $P_N^N(\mathbf{r}) = u_0(\mathbf{r}) + f_N[u_1(\mathbf{r}), u_2(\mathbf{r}), \dots]$ , where  $f_N$  is a function independent of the incident field  $u_0(\mathbf{r})$ . Since we are mainly interested in the properties of the scattered field, all the results displayed below refer to  $[P_N^N(\mathbf{r}) - u_0(\mathbf{r})]/(e^{ikr}/r) = \tilde{P}_N^N(\mathbf{r})$ , where  $\tilde{P}_N^N(\mathbf{r})$  is the approximant for the scattered field amplitude. In other words, all Padé approximants are of the form

$$P_N^N(\mathbf{r}) = u_0(\mathbf{r}) + \frac{e^{ikr}}{r} \tilde{P}_N^N(\mathbf{r}), \quad (17)$$

where  $\tilde{P}_N^N(\mathbf{r})$  is independent of  $r$ .

Figure 2 shows the plot of  $|\tilde{P}_N^N(\mathbf{r})|$  for  $N = 1, 2$ , and 3. In the scale used, the lines for the approximants are indistinguishable from the line representing the exact solution. This amazing match is due to the fact that the exact solution is already in a Padé form, being represented by a fraction of two second-degree polynomials in the variable  $\sigma$ . The truly remarkable thing to note here is that only two coefficients ( $\tilde{u}_1$  and  $\tilde{u}_2$ ) are necessary to construct  $P_1^1$ , which agrees with the exact answer in ten decimal places for some values of  $\alpha$  (or  $\sigma$ ).

Table II compares the exact solution with its Padé and Taylor representations for a fixed scattering direction.

In this Hermitian configuration we expect the scattered radiation field to possess a symmetric profile in relation to the scatterers. Figure 3 shows the plot of the scattered field amplitude as a function of the polar angle  $\theta$ . Again, the first Padé approximant  $\tilde{P}_1^1$  is able to retrieve information about the scattering directions from the exact solution by using only two coefficients of the Taylor series. The figure also displays the first, second, and third Born approximations along with the exact solution to the problem. The plotted lines of  $|\tilde{P}_1^1(\mathbf{r})|$ ,  $|\tilde{P}_2^2(\mathbf{r})|$ , and  $|\tilde{u}_s(\mathbf{r})|$  are indistinguishable from one another in the scale adopted (black curve).

### B. Non-Hermitian scattering

Consider now an active  $\mathcal{PT}$  dipole with balanced gain and loss ( $\gamma \neq 0$ ). This system has been studied under the first Born approximation [35,36]. The first thing to note is that we can no longer consider  $\sigma$  or  $\gamma$  as an expansion parameter since we are unable to recover the unperturbed problem (no scatterers) by letting  $\sigma$  or  $\gamma$  vanish independently. By the same reasoning as in the Hermitian case, we ask what happens to the scattered field amplitude for a fixed direction as we increase  $\sigma$  or  $\gamma$ . Figure 4 displays the behavior of the exact solution, the Padé approximants, and the Taylor summation

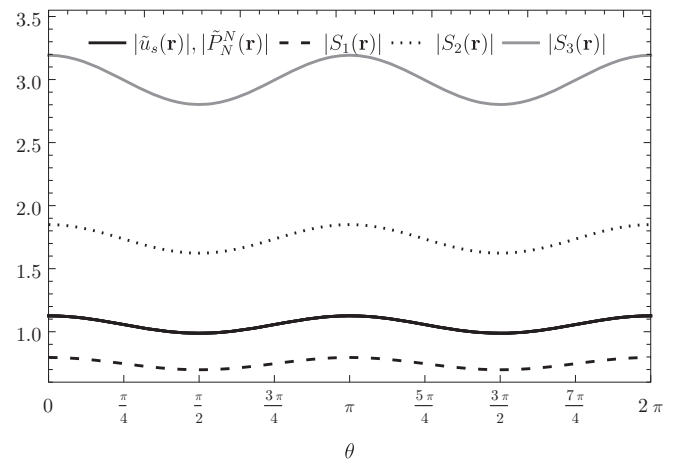


FIG. 3. Scattered field amplitude as a function of  $\theta$ . The dashed line shows the first Born approximation  $|S_1(\mathbf{r})|$ , the dotted line  $|S_2(\mathbf{r})|$ , the gray solid line  $|S_3(\mathbf{r})|$ , and the black solid line  $|\tilde{P}_N^N(\mathbf{r})|$  ( $N = 1, 2, 3$ ) and the exact solution  $|\tilde{u}_s(\mathbf{r})|$ . The parameters are  $\phi = 0$ ,  $k = 1$ ,  $x_0 = \frac{1}{2}$ ,  $\sigma = 5$ , and  $\gamma = 0$ . All quantities plotted have arbitrary units.

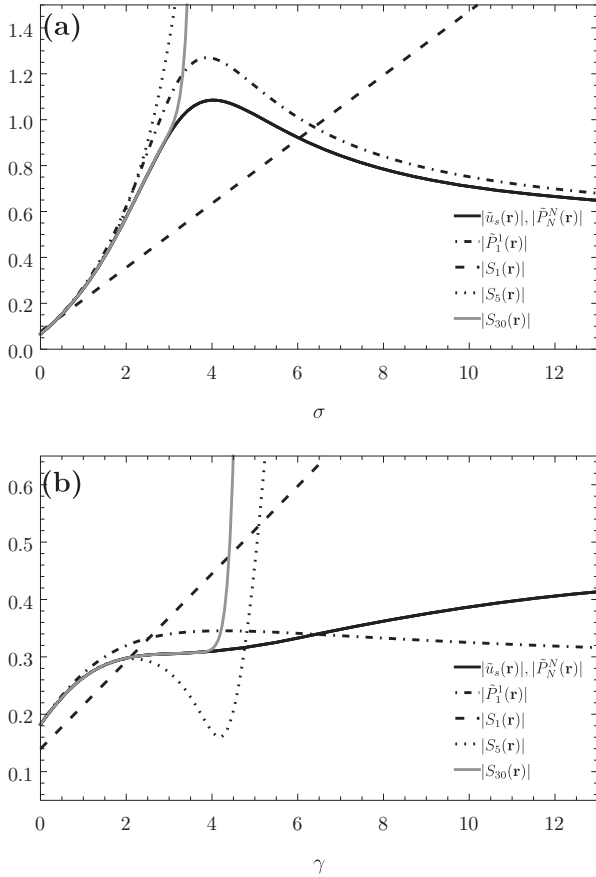


FIG. 4. (a) Same as in Fig. 2 but with  $\gamma = 1$  and (b)  $|\tilde{u}_s(\mathbf{r})|$ ,  $|S_1(\mathbf{r})|$ ,  $|S_5(\mathbf{r})|$ ,  $|S_{30}(\mathbf{r})|$ ,  $|\tilde{P}_1^1(\mathbf{r})|$ , and  $|\tilde{P}_N^N(\mathbf{r})|$  ( $N = 2, 3$ ) as a function of  $\gamma$  with  $\sigma = 1$ . The parameters are  $\theta = \frac{\pi}{2}$ ,  $\phi = 0$ ,  $k = 1$ , and  $x_0 = \frac{1}{2}$ . The line plots of  $|\tilde{P}_2^2(\mathbf{r})|$  and  $|\tilde{P}_3^3(\mathbf{r})|$  are indistinguishable from the line representing the exact solution. All quantities plotted have arbitrary units.

as a function of  $\sigma$  (for  $\gamma = 1$ ) in Fig. 4(a) and as a function of  $\gamma$  (for  $\sigma = 1$ ) in Fig. 4(b). In this case, even though the closed-form solution is already in Padé form, the  $\tilde{P}_1^1$  approximant is not able to return accurate results, as the dot-dashed curve in Fig. 4 demonstrates. However, the second diagonal Padé approximant  $\tilde{P}_2^2$  agrees almost exactly with the correct answer, its plotted line being indistinguishable from the line of  $|\tilde{u}_s|$

(black curve). Thus, with only four coefficients of the Born series, it is possible to obtain very accurate results by varying  $\sigma$  and/or  $\gamma$ . We conclude that Padé approximants also work for dielectric systems with gain. To explain the behavior of the partial sums  $S_N$ , the reader can consult Table III, which shows the radius of convergence in the complex  $\alpha$  plane for several values of  $\gamma$  and  $\sigma$ . For example, by inspecting Table III one can explain the divergence of  $S_N$  in Fig. 4(a) for  $\sigma \approx 3.5$ . This table also suggests one general behavior, that is, increasing  $\gamma$  decreases  $R_\alpha$ . Thus, gain and loss directly influence the radius of convergence of the Born series.

Physically, as the gain and loss parameter  $\gamma$  increases, the scattered field amplitude saturates to a constant value independent of  $\sigma$ . This can be verified by inspecting Eq. (13) in the limit  $\gamma \rightarrow \infty$ , which gives

$$\tilde{u}_s(\mathbf{r}) \sim r_0 \cos(kr_0 \sin \theta) [i \tan(kr_0) - 1]. \quad (18)$$

Since the Born approximation is formed by retaining the first term in the Taylor expansion, it predicts an infinite amount of energy to the scattered radiation when  $\gamma$  (or  $\sigma$ ) increases, which is clearly nonphysical. Curiously, we also verified that in this limit, the scattered field profile turns out to be symmetric in the sense that it scatters light like its Hermitian counterpart (the scattered field amplitude being an even function of  $\theta$ ). Thus, even though the system is non-Hermitian in character, it can generate a scattered field with symmetrical properties.

Regarding the directional properties of the scattered radiation, Fig. 5 shows the non-Hermitian version of Fig. 3. It is seen that the symmetric character of the field is broken as a result of the gain and loss present in the scatterer. In general, more radiation is emitted in the direction where the scatterer with gain is located ( $\theta = \frac{\pi}{2}$ ,  $\phi = 0$ ). The first diagonal Padé approximant  $\tilde{P}_1^1$  is again not accurate enough to represent the analytical solution. On the other hand, the second diagonal Padé approximant  $\tilde{P}_2^2$  displays remarkable agreement with the exact solution  $|\tilde{u}_s|$  in the far zone. All high-order Padé approximants  $\tilde{P}_N^N$  for  $N > 3$  give even more accurate numerical values. In order to expose some numerical values from this remarkable match between  $\tilde{P}_N^N$  and  $|\tilde{u}_s|$ , Table IV demonstrates the agreement between partial sums  $S_N$ , Padé approximants  $\tilde{P}_N^N$ , and the closed-form expression  $|\tilde{u}_s|$  for several values of  $\alpha$ .

TABLE III. Radius of convergence in the complex  $\alpha$  plane for the Taylor series  $\sum_n u_n \alpha^n$  for several values of  $\sigma$  and  $\gamma$ . The parameters are  $\phi = 0$ ,  $\theta = \pi/2$ ,  $k = 1$ , and  $x_0 = 0.5$ .

$\sigma$	$R_\alpha(\gamma = 1)$	$R_\alpha(\gamma = 5)$	$R_\alpha(\gamma = 10)$
1	2.86615	0.909877	0.471608
2	1.68626	0.827169	0.454939
3	1.1624	0.736475	0.435248
4	0.881973	0.64986	0.413585
5	0.709336	0.57323	0.39096
6	0.592808	0.508002	0.368237
7	0.508995	0.453362	0.346077
8	0.445866	0.407738	0.32493
9	0.396627	0.369507	0.305066
10	0.357158	0.337251	0.286615

TABLE IV. Comparison between the exact solution  $\tilde{u}_s$  for the scattered field amplitude and its Taylor  $S_N$  and Padé  $\tilde{P}_N^N$  representations (with  $\sigma = 1$  and  $\gamma = 1$ ). The parameters are  $k = 1$ ,  $x_0 = \frac{1}{2}$ ,  $\phi = 0$ , and  $\theta = \frac{\pi}{2}$ . All values of  $\alpha$  are inside the radius of convergence.

$\alpha$	Exact solution	$ S_N  (N)$	$ \tilde{P}_1^1 $	$ \tilde{P}_2^2 $	$ \tilde{P}_3^3 $
2.86	0.7033410417066716	0.7043237092362864(3000)	1.008376895441823	0.7033410417066689	0.7049399474872458
1.43	0.3980343662336995	0.3980343662336992(100)	0.42667412501982227	0.3980343662336992	0.39814262254852434
0.725	0.18228544344617278	0.18228544344617276(30)	0.1848242433424334	0.18228544344617276	0.18229087198641047
0.0725	0.015913207781144273	0.01591320778114422(10)	0.015914968978725994	0.015913207781144276	0.0159132081952227

In closing, a few remarks about Padé approximants are in order. We have emphasized that the approximants become very close to the actual answer but we have not proved such a claim. This is a very difficult question since there are no theorems on the convergence and uniqueness of Padé approximants in the general case for an arbitrary function [11]. There is only one class of functions for which the Padé approximants are known to converge to the exact answer and that is the class of Stieltjes functions. However, there is evidence that the approximants converge to the exact answer (in this scattering scenario at least) and our results suggest that this indeed happens [21]. A more formal and general discussion in this

direction, involving light field amplitudes satisfying Eq. (1), is still lacking in the literature.

#### IV. CONCLUSION

We have studied the scattering of a monochromatic plane wave by a  $\mathcal{PT}$ -symmetric dipole. An explicit closed-form expression for the scattered wave amplitude in the far-zone was obtained. The Padé approximants and the Born approximation were compared with the closed-form expression and we stressed the limitations of the Born series in the strong-scattering regime. The Padé approximants were shown to be a remarkable and accurate alternative for treating weak- and strong-scattering regimes. The approach using Padé approximants may be more suitable for problems that do not have an exact solution and when the Born series diverge. Therefore, we believe that our results contribute an important step towards scattering in strong regimes.

One possible experimental implementation of our scattering system could be realized as in Ref. [37], consisting of a photonic structure with holes filled by semiconductor junctions, as also suggested in Ref. [35].

#### ACKNOWLEDGMENTS

The authors would like to acknowledge financial support from CNPq.

#### APPENDIX: CLOSED-FORM EXPRESSION FOR $\tilde{u}_s(\mathbf{r})$

In this Appendix we demonstrate the induction process used to obtain a closed-form expression for  $\tilde{u}_s$  and  $u_n$  in terms of  $u_0$ . Starting from Eq. (11), the explicit form for the first three corrections are given by

$$u_1(\mathbf{r}) = \frac{k^2}{4\pi} \frac{e^{ikr}}{r} [P_0 e^{-ik\hat{s}\cdot\mathbf{r}_0} + Q_0 e^{ik\hat{s}\cdot\mathbf{r}_0}], \quad (A1)$$

where  $P_0 = (\sigma + i\gamma)e^{ik\hat{a}\cdot\mathbf{r}_0}$  and  $Q_0 = (\sigma - i\gamma)e^{-ik\hat{a}\cdot\mathbf{r}_0}$ ;

$$u_2(\mathbf{r}) = \left(\frac{k^2}{4\pi}\right)^2 \frac{e^{ikr}}{r} [P_1 e^{-ik\hat{s}\cdot\mathbf{r}_0} + Q_1 e^{ik\hat{s}\cdot\mathbf{r}_0}], \quad (A2)$$

where  $P_1 \equiv (\sigma + i\gamma)(P_0 + Q_0 e^{2ikr_0})/r_0$  and  $Q_1 \equiv (\sigma - i\gamma)(P_0 e^{2ikr_0} + Q_0)/r_0$ ; and

$$u_3(\mathbf{r}) = \left(\frac{k^2}{4\pi}\right)^3 \frac{e^{ikr}}{r} [P_2 e^{-ik\hat{s}\cdot\mathbf{r}_0} + Q_2 e^{ik\hat{s}\cdot\mathbf{r}_0}], \quad (A3)$$

where  $P_2 \equiv (\sigma + i\gamma)(P_1 + Q_1 e^{2ikr_0})/r_0$  and  $Q_2 \equiv (\sigma - i\gamma)(P_1 e^{2ikr_0} + Q_1)/r_0$ . Thus, the general formula for  $u_n$  can

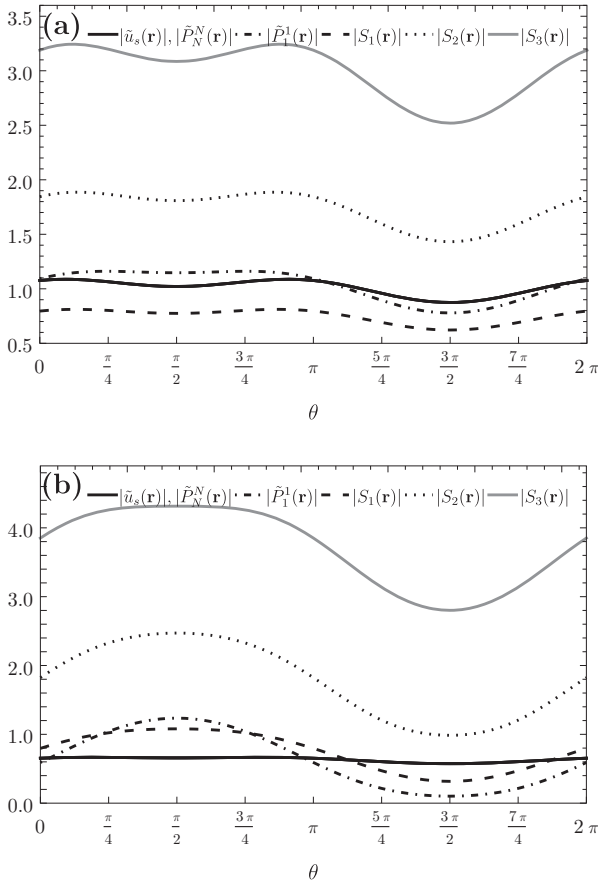


FIG. 5. (a) Same as in Fig. 3 but with  $\sigma = 5$  and  $\gamma = 1$  and (b)  $\gamma = 5$ , for  $|\tilde{u}_s(\mathbf{r})|$ ,  $|S_1(\mathbf{r})|$ ,  $|S_2(\mathbf{r})|$ ,  $|S_3(\mathbf{r})|$ ,  $|\tilde{P}_1^1(\mathbf{r})|$ , and  $|\tilde{P}_N^N(\mathbf{r})|$  ( $N = 2, 3$ ) as a function of  $\theta$ . The parameters are  $\phi = 0$ ,  $k = 1$ , and  $x_0 = \frac{1}{2}$ . The line plots of  $|\tilde{P}_2^2(\mathbf{r})|$  and  $|\tilde{P}_3^3(\mathbf{r})|$  are indistinguishable from the line representing the exact solution. All quantities plotted have arbitrary units.

be written as

$$u_n(\mathbf{r}) = \left(\frac{k^2}{4\pi}\right)^n \frac{e^{ikr}}{r} [P_{n-1}e^{-ik\hat{s}\cdot\mathbf{r}_0} + Q_{n-1}e^{ik\hat{s}\cdot\mathbf{r}_0}], \quad (\text{A4})$$

where

$$\begin{aligned} P_n &= D_1 P_{n-1} + D_2 Q_{n-1}, \\ Q_n &= D_3 P_{n-1} + D_4 Q_{n-1}, \end{aligned} \quad (\text{A5})$$

with  $D_1 = (\sigma + i\gamma)/r_0$ ,  $D_2 = (\sigma + i\gamma)e^{2ki r_0}/r_0$ ,  $D_3 = (\sigma - i\gamma)e^{2ki r_0}/r_0$ , and  $D_4 = (\sigma - i\gamma)/r_0$ . Equations (A5) represent a system of difference equations with constant coefficients and initial conditions  $P_0 = (\sigma + i\gamma)e^{ik\hat{a}\cdot\mathbf{r}_0}$  and  $Q_0 = (\sigma - i\gamma)e^{-ik\hat{a}\cdot\mathbf{r}_0}$ . They can be solved by writing the system as

$$\begin{bmatrix} P_n \\ Q_n \end{bmatrix} = \begin{bmatrix} D_1 & D_2 \\ D_3 & D_4 \end{bmatrix}^n \begin{bmatrix} P_0 \\ Q_0 \end{bmatrix} = D^n \begin{bmatrix} P_0 \\ Q_0 \end{bmatrix}, \quad (\text{A6})$$

where  $D$  is a  $2 \times 2$  matrix with coefficients  $D_j$ . By using the identity

$$D^n = \frac{\lambda_1^n - \lambda_2^n}{\lambda_1 - \lambda_2} D - \lambda_1 \lambda_2 \frac{\lambda_1^{n-1} - \lambda_2^{n-1}}{\lambda_1 - \lambda_2} 1, \quad (\text{A7})$$

where  $\lambda_1$  and  $\lambda_2$  are the eigenvalues of  $D$  and  $1$  is the identity matrix, the general solution is given explicitly by

$$\begin{aligned} P_n &= \frac{2^{-n-1}}{\sqrt{(D_1 - D_4)^2 + 4D_2 D_3}} \\ &\times ((D_1 P_0 + 2D_2 Q_0 - D_4 P_0) \\ &\times \{[\sqrt{(D_1 - D_4)^2 + 4D_2 D_3} + D_1 + D_4]^n \\ &- [-\sqrt{(D_1 - D_4)^2 + 4D_2 D_3} + D_1 + D_4]^n\} \\ &+ P_0 \sqrt{(D_1 - D_4)^2 + 4D_2 D_3} \\ &\times \{[-\sqrt{(D_1 - D_4)^2 + 4D_2 D_3} + D_1 + D_4]^n \\ &+ [\sqrt{(D_1 - D_4)^2 + 4D_2 D_3} + D_1 + D_4]^n\}), \quad (\text{A8}) \\ Q_n &= \frac{2^{-n-1}}{\sqrt{(D_1 - D_4)^2 + 4D_2 D_3}} \\ &\times ((D_4 Q_0 + 2D_3 P_0 - D_1 Q_0) \end{aligned}$$

$$\begin{aligned} &\times \{[\sqrt{(D_1 - D_4)^2 + 4D_2 D_3} + D_1 + D_4]^n \\ &- [-\sqrt{(D_1 - D_4)^2 + 4D_2 D_3} + D_1 + D_4]^n\} \\ &+ Q_0 \sqrt{(D_1 - D_4)^2 + 4D_2 D_3} \\ &\times \{[-\sqrt{(D_1 - D_4)^2 + 4D_2 D_3} + D_1 + D_4]^n \\ &+ [\sqrt{(D_1 - D_4)^2 + 4D_2 D_3} + D_1 + D_4]^n\}). \quad (\text{A9}) \end{aligned}$$

Equations (A8) and (A9) together with (A4) represent the general solution for the Born series. The total wave field is given by the sum of the incident and scattered waves (with  $\alpha = 1$ ),

$$u(\mathbf{r}) = u_0(\mathbf{r}) + \sum_{n=1}^{\infty} u_n(\mathbf{r}), \quad (\text{A10})$$

where, after substituting Eq. (A4) into Eq. (A10), we obtain

$$\begin{aligned} u(\mathbf{r}) &= u_0(\mathbf{r}) + \frac{e^{ikr}}{r} \sum_{n=1}^{\infty} \left(\frac{k^2}{4\pi}\right)^n \\ &\times (P_{n-1}e^{-ik\hat{s}\cdot\mathbf{r}_0} + Q_{n-1}e^{ik\hat{s}\cdot\mathbf{r}_0}). \quad (\text{A11}) \end{aligned}$$

It is easy to see that all the summation terms in Eq. (A11) can be put into a geometric series form  $\sum_{n=1}^{\infty} \zeta^n = \frac{\zeta}{1-\zeta}$ , with  $|\zeta| < 1$ . Thus, (A11) can be written as

$$u(\mathbf{r}) = u_0(\mathbf{r}) + \frac{e^{ikr}}{r} \tilde{u}_s(\mathbf{r}), \quad (\text{A12})$$

where

$$\begin{aligned} \tilde{u}_s(\mathbf{r}) &= e^{-ik\hat{s}\cdot\mathbf{r}_0} \\ &\times \frac{-D_2 k^4 Q_0 + D_4 k^4 P_0 - 4\pi k^2 P_0}{D_2 D_3 k^4 - (D_1 k^2 - 4\pi)(D_4 k^2 - 4\pi)} \\ &+ e^{ik\hat{s}\cdot\mathbf{r}_0} \\ &\times \frac{D_1 k^4 Q_0 - D_3 k^4 P_0 - 4\pi k^2 Q_0}{D_2 D_3 k^4 - (D_1 k^2 - 4\pi)(D_4 k^2 - 4\pi)} \quad (\text{A13}) \end{aligned}$$

is the closed-form expression for the scattered wave in the far-zone approximation.

- 
- [1] R. G. Newton, *Scattering Theory of Waves and Particles* (Springer Science + Business Media, New York, 2013).
- [2] I. R. Lapidus, *Am. J. Phys.* **37**, 1064 (1969).
- [3] R. Kleinman, G. Roach, and P. van den Berg, *J. Opt. Soc. Am. A* **7**, 890 (1990).
- [4] O. J. Martin, A. Dereux, and C. Girard, *J. Opt. Soc. Am. A* **11**, 1073 (1994).
- [5] T. Shirai and T. Asakura, *Opt. Commun.* **123**, 234 (1996).
- [6] A. Abubakar and T. M. Habashy, *Wave Motion* **41**, 211 (2005).
- [7] S. Trattner, M. Feigin, H. Greenspan, and N. Sochen, *J. Opt. Soc. Am. A* **26**, 1147 (2009).
- [8] T. Setälä, T. Hakkarainen, A. T. Friberg, and B. J. Hoenders, *Phys. Rev. A* **82**, 013814 (2010).
- [9] J. Lim, H. Ding, M. Mir, R. Zhu, K. Tangella, and G. Popescu, *Biomed. Opt. Express* **2**, 2784 (2011).
- [10] A. S. Bereza, A. V. Nemykin, S. V. Perminov, L. L. Frumin, and D. A. Shapiro, *Phys. Rev. A* **95**, 063839 (2017).
- [11] G. A. Baker, Jr., *Essentials of Padé Approximants* (Elsevier, Amsterdam, 1975).
- [12] C. Brezinski, *History of Continued Fractions and Padé Approximants* (Springer Science + Business Media, New York, 2012), Vol. 12.
- [13] C. M. Bender and S. A. Orszag, *Advanced Mathematical Methods for Scientists and Engineers I: Asymptotic Methods and Perturbation Theory* (Springer Science + Business Media, New York, 2013).
- [14] S. Tani, *Phys. Rev.* **139**, B1011 (1965).
- [15] J. Gammel and F. McDonald, *Phys. Rev.* **142**, 1245 (1966).
- [16] I. R. Lapidus, *Am. J. Phys.* **48**, 51 (1980).
- [17] J. Tjon, *Phys. Rev. D* **1**, 2109 (1970).
- [18] J. Fleischer and M. Pindor, *Phys. Rev. D* **24**, 1978 (1981).

- [19] C. Eftimiu and G. Welland, *IEEE Trans. Antennas Propag.* **35**, 721 (1987).
- [20] G. R. Hadley, *Opt. Lett.* **17**, 1426 (1992).
- [21] T. A. van der Sijs, O. El Gawhary, and H. P. Urbach, *Phys. Rev. Research* **2**, 013308 (2020).
- [22] C. M. Bender and S. Boettcher, *Phys. Rev. Lett.* **80**, 5243 (1998).
- [23] C. M. Bender, *Rep. Prog. Phys.* **70**, 947 (2007).
- [24] C. E. Rüter, K. G. Makris, R. El-Ganainy, D. N. Christodoulides, M. Segev, and D. Kip, *Nat. Phys.* **6**, 192 (2010).
- [25] S. Longhi, *Europhys. Lett.* **120**, 64001 (2018).
- [26] Y. D. Chong, L. Ge, and A. D. Stone, *Phys. Rev. Lett.* **106**, 093902 (2011).
- [27] P. Ambichl, K. G. Makris, L. Ge, Y. Chong, A. D. Stone, and S. Rotter, *Phys. Rev. X* **3**, 041030 (2013).
- [28] P. A. Kalozoumis, G. Pappas, F. K. Diakonous, and P. Schmelcher, *Phys. Rev. A* **90**, 043809 (2014).
- [29] S. Longhi and L. Feng, *Opt. Lett.* **39**, 5026 (2014).
- [30] P. Kalozoumis, C. Morfonios, G. Kodaxis, F. Diakonous, and P. Schmelcher, *Appl. Phys. Lett.* **110**, 121106 (2017).
- [31] V. Achilleos, Y. Aurégan, and V. Pagneux, *Phys. Rev. Lett.* **119**, 243904 (2017).
- [32] L. Feng, Y.-L. Xu, W. S. Fegadolli, M.-H. Lu, J. E. Oliveira, V. R. Almeida, Y.-F. Chen, and A. Scherer, *Nat. Mater.* **12**, 108 (2013).
- [33] S. Longhi, *Phys. Rev. A* **82**, 031801(R) (2010).
- [34] P. Markos and C. M. Soukoulis, *Wave Propagation: From Electrons to Photonic Crystals and Left-Handed Materials* (Princeton University Press, Princeton, 2008).
- [35] K. Staliunas, P. Markoš, and V. Kuzmiak, *Phys. Rev. A* **96**, 043852 (2017).
- [36] P. A. Brandão and S. B. Cavalcanti, *Phys. Rev. A* **100**, 043822 (2019).
- [37] M. Turduev, M. Botey, I. Giden, R. Herrero, H. Kurt, E. Ozbay, and K. Staliunas, *Phys. Rev. A* **91**, 023825 (2015).